

ICSV14
Cairns • Australia
9-12 July, 2007



MOMENT CONTROL OF THE SOUND RADIATED FROM AN AXIALLY EXCITED CYLINDRICAL SHELL

James A. Forrest

Maritime Platforms Division, Defence Science & Technology Organisation, PO Box 4331, Melbourne
VIC 3001, Australia.

james.forrest@dsto.defence.gov.au

Abstract

This paper explores the feasibility of using moments to control the sound radiated from a small cylindrical shell. Previous theoretical work has shown that a circumferential line moment can provide good control of radiated sound in the first three axisymmetric axial modes of a water-loaded cylindrical shell representing a generic submarine. The results described here are part of a study that seeks to experimentally validate the theoretical result on a smaller scale in air. The steel shell considered is 1.5 m long, 400 mm in diameter and 2 mm thick. Its ends are capped by 20 mm thick circular steel plates. One end-plate would be driven by a shaker, with the proposed control moment provided by piezo stack actuators acting on a T-section ring-stiffener. The stack forces are modelled as two circumferential line forces, and a modal approach with cylindrical shell equations is used to calculate their optimum value to control sound radiation at axial resonance. Although some reduction in radiated sound from the shell in air is possible, the problem is complicated by the requirement for large control forces and a number of higher-order circumferential modes with resonances close to the axisymmetric ones being controlled.

1. INTRODUCTION

Minimisation of the sound radiated from a naval submarine is essential to reduce its detectability and thereby maximise its effectiveness. Since most submarines are cylindrical in shape, many investigations are based on relatively simple cylindrical shell structures. Much early work on shells and cylindrical shells in particular is summarised by Leissa [1]. Hodges et al. [2] present a detailed model for vibration transmission in a ribbed cylinder that also models the internal degrees of freedom and resonances of the ribs. The wave propagation in periodically stiffened shells, with its pass and stop bands, is modelled using a finite-element approach by Solaroli et al. [3] and by an analytical technique by Lee and Kim [4]. Fluid loading has a big effect on the response of a submerged structure. Scott [5] presents a comprehensive analysis of the free modes of propagation for an infinitely long thin cylindrical shell with fluid loading. Harari and Sandman [6] consider the acoustic radiation from the shell as well. Choi et al. [7] use a modal-based method to model the vibration and acoustic radiation of submerged cylindrical shells that include internal substructures.

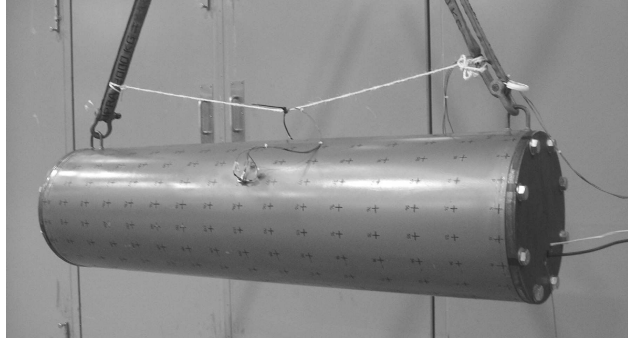


Figure 1. The cylindrical shell with heavy end plates.

Numerical approaches can model more general structures than can be treated by analytical means. Marcus and Houston [8] use a finite-element (FE) model to show that the addition of point masses to the internal frames of a submerged cylindrical shell increases its acoustic radiation by coupling high and low order circumferential resonances. Homm et al. [9] use both FE analysis alone and FE combined with the boundary-element (BE) method to model the structural and acoustic response of two joined hemispherically capped cylinders with some internal structure. Blakemore et al. [10] model a fluid-loaded ribbed cylindrical shell with an extended form of statistical energy analysis (SEA) that can deal with the periodicity of the structure as well as higher frequencies than FE. While these methods can give good results, they are too numerically intensive for real-time use in active control where a simple cost function for radiated sound is needed. Fuller et al. [11] discuss active vibration control of cylindrical shells, including active structural acoustic control to minimise the structure-borne radiated sound.

A simplified analytical radiation model for a submarine is described in Pan et al. [12]. It considers low-frequency axial excitation, as might be induced by the propeller shaft on the thrust block of a submarine. Only axisymmetric motion is considered, since the ‘concertina’ (predominantly axial) modes are of most interest. The sound radiation due to these modes is shown to be controlled by a circumferential moment which is relatively small compared to the axial force. Figure 1 shows the small-scale cylinder considered in this paper as a potential test-bed to experimentally validate this moment control. An initial modal survey of the cylinder is given in Forrest [13], which shows that the natural frequencies up to at least 600 Hz can be predicted within a few per cent by simple Donnell-Mushtari shell theory for a cylinder with shear-diaphragm (simple support) end conditions, despite the end caps which add mass and provide a built-in type boundary. This is because the modes in question are mainly radial, with little end motion. This paper will investigate the feasibility of moment control of the radiated sound from the small-scale cylinder in axisymmetric motion.

2. MODELLING

A thin cylindrical shell of radius a , thickness h and length L is shown in Fig. 2(a). The Donnell-Mushtari equations of motion for such a shell can be determined from Leissa [1] and are

$$\begin{aligned}
 a^2 u_{xx} + (1-\nu)u_{\theta\theta}/2 - \rho(1-\nu^2)a^2 \ddot{u}/E + (1+\nu)av_{x\theta}/2 + \nu aw_x + a^2(1-\nu^2)q_1/Eh &= 0 \\
 (1+\nu)av_{x\theta}/2 + (1-\nu)a^2 v_{xx}/2 + v_{\theta\theta} - \rho a^2(1-\nu^2)\ddot{v}/E + w_\theta + a^2(1-\nu^2)q_2/Eh &= 0 \\
 \nu au_x + v_\theta + w + h^2 \nabla^4 w/12a^2 + \rho a^2(1-\nu^2)\ddot{w}/E - a^2(1-\nu^2)q_3/Eh &= 0
 \end{aligned} \tag{1}$$

where u , v and w are the displacements and q_1 , q_2 and q_3 are the net external surface tractions in the x , y and z directions respectively; ρ is the density, E the Young's modulus and ν the Poisson's ratio of the shell material; and subscripts x and θ denote differentiation with respect to those variables and dot indicates differentiation with respect to time. Solutions which satisfy shear-diaphragm boundary conditions are

$$u = A \cos(m\pi x/L) \cos n\theta e^{i\omega t}, \quad v = B \sin(m\pi x/L) \sin n\theta e^{i\omega t}, \quad w = C \sin(m\pi x/L) \cos n\theta e^{i\omega t} \quad (2)$$

which when substituted in Eq. (1) with zero external forces give a cubic characteristic equation in the natural frequency squared ω^2 for a given combination of m and n . This can be solved as described by Forrest [13], with non-axisymmetric motion ($n \geq 1$) dominating the lower modes of the cylinder in Fig. 1.

For the axisymmetric ($n=0$) vibration of interest in submarines, all derivatives with respect to θ in Eqs. (1) are zero, and the second equation decouples v from the other two in u and w . The equation in v describes torsional modes which are not of concern here. Consider instead the axial and radial response of the cylinder shown schematically in Fig. 2(b). F_1 is the axial excitation force that would be provided by an inertial actuator, F_c are control line forces which would be provided by piezo stacks acting on a T-stiffener, and M_1 and M_2 are the masses of the end plates, assumed rigid. The axial and radial force distributions are

$$\begin{aligned} q_1 &= F_1 \delta(x)/2\pi a - M_1 \ddot{u}|_{x=0} \delta(x)/2\pi a - M_1 \ddot{u}|_{x=L} \delta(x-L)/2\pi a \\ q_3 &= -F_c \delta(x-d_1) + F_c \delta(x-d_2) \end{aligned} \quad (3)$$

where division by $2\pi a$ distributes the point forces around the circumference and the Dirac delta functions $\delta(x)$ distribute all the forces along the cylinder's length. While a wave solution as used by Pan et. al [12] may seem initially attractive, using solutions of the form $e^{\lambda x/a} e^{i\omega t}$ for both u and w , some of the roots λ for the parameter values used here result in extremely large exponentials which are numerically intractable. Thus a modal solution will be used, based on the forms in Eq. (2), given that the cylindrical shell to be modelled was found in Forrest [13] to be well-described by these functions even if its boundary conditions do not strictly adhere to shear-diaphragm ones. The inertial forces due to the end plates are now included in the forces of Eq. (3), so this assumption only violates the zero slope end condition. As there is no θ dependence, the responses can be written as the modal sums

$$u = \sum_{j=1}^{\infty} A_j \cos(j\pi x/L) e^{i\omega t} = U e^{i\omega t}, \quad w = \sum_{j=1}^{\infty} C_j \sin(j\pi x/L) e^{i\omega t} = W e^{i\omega t} \quad (4)$$

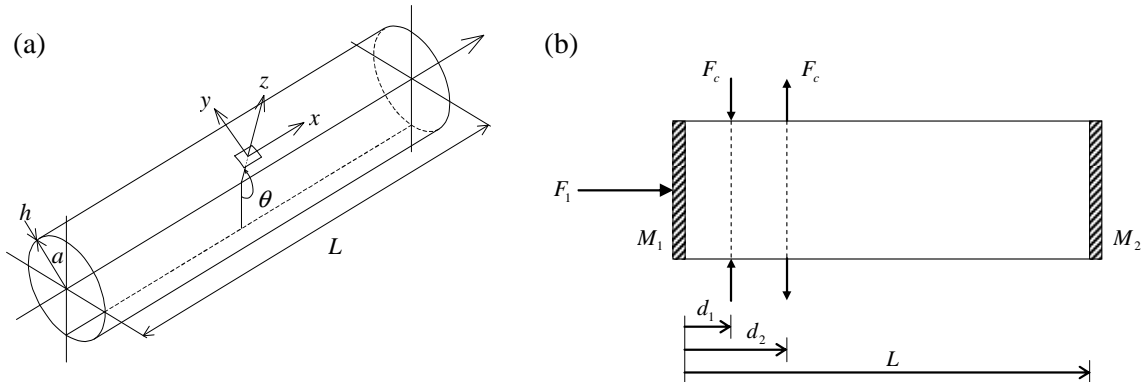


Figure 2. (a) A thin cylindrical shell of radius a , thickness h and length L , showing the coordinate system x , y and z . (b) Schematic side view of the cylindrical shell with rigid heavy end plates showing the axial driving force and pair of line control forces.

where in practice only as many terms as needed for convergence need to be summed.

A solution can be found by using the orthogonality of the mode-shape functions to consider the contribution of mode m alone to the displacements in Eq. (4) and forces in Eq. (3). Substituting into the axisymmetric version of Eqs. (1), multiplying by $\cos(m\pi x/L)$ or $\sin(m\pi x/L)$ and integrating over the length $[0, L]$ to remove the x -dependence yields the matrix equation

$$\begin{bmatrix} -\lambda_m^2 + \left(1 + \frac{M_1 + M_2}{\pi \rho a h L}\right) \Omega^2 & v \lambda_m \\ -v \lambda_m & 1 + k \lambda_m^4 - \Omega^2 \end{bmatrix} \begin{bmatrix} A_m \\ C_m \end{bmatrix} = \begin{bmatrix} \frac{-a(1-v^2)}{\pi E h L} F_1 \\ \frac{-2a^2(1-v^2)}{E h L} \left(\sin \frac{\lambda_m d_1}{a} - \sin \frac{\lambda_m d_2}{a} \right) F_c \end{bmatrix} \quad (5)$$

where $\Omega^2 \equiv \rho(1-v^2)a^2\omega^2/E$, $\lambda_m \equiv m\pi a/L$ and $k \equiv h^2/12a^2$. The free vibration problem for the cylinder with added massive end plates can be solved by setting $F_1 = F_c = 0$ and solving the characteristic determinant of the matrix on the left-hand side for Ω^2 . This results in two natural frequencies for each m , one largely axial (the ‘concertina’ mode) and one largely radial (the ‘breathing’ or ‘ring’ mode). For forced vibration, some damping is included and $[A_m \ C_m]^T$ is calculated from (5) for a range of m and ω values, and substituted into Eqs. (4). Loss-factor damping of η will be used such that E is replaced by $E(1+i\eta)$.

In order to develop a cost function for the sound radiation, each end plate can be considered as a piston in the end of a tube and the shell as a cylindrical radiator. The interaction between the three sound sources that therefore make up the cylinder is ignored for simplicity. Bies and Hansen [14] give results for the piston and Fahy [15] gives results for infinitely long cylindrical radiators. The radiated sound power P_{piston} for the piston and power per unit length $\bar{P}_{cylinder}$ for the cylinder, when the radiation efficiencies are unity, are given by

$$P_{piston} = \pi a^2 \rho_o c_o |V|^2 / 2 \quad \text{and} \quad \bar{P}_{cylinder} = 2\pi a \rho_o c_o \langle \bar{V}^2 \rangle \quad (6)$$

where ρ_o is the density of and c_o the speed of sound in the acoustic medium. If V is complex velocity amplitude, $|V|^2 = V \cdot V^*$ is the squared velocity magnitude of the piston, and $\langle \bar{V}^2 \rangle$ the space average of $V \cdot V^*/2$, the time-averaged mean-square normal velocity of the cylinder’s surface, where asterisk $*$ indicates complex conjugate. For the end caps, $V = i\omega U$ at $x=0$ and $x=L$, while for the cylindrical shell, $V = i\omega W$. This with the displacements in Eq. (4) can be substituted into Eqs. (6) to give the total sound power radiated from the cylinder as

$$P_{total} = \frac{1}{2} \rho_o c_o \pi a \omega^2 \left(a \sum_{j=1}^{\infty} \sum_{k=1}^{\infty} (1 + (-1)^{j+k}) A_j A_k^* + L \sum_{j=1}^{\infty} C_j C_j^* \right) \quad (7)$$

where the cross terms in the double sum only affect the power level between resonances. The power can be expressed as a dB sound power level (PWL) with a reference power of 10^{-12} W.

At resonance of a mode m , the sound power is dominated by that mode’s terms. To find the optimum line forces to control a resonance, only the terms for mode m in Eq. (7) are therefore considered. The mode’s coefficients A_m and C_m can be found in terms of F_1 and F_c analytically or numerically from Eq. (5) by inverting the 2×2 matrix. Writing these as

$$A_m = \alpha F_1 + \beta F_c \quad \text{and} \quad B_m = \gamma F_1 + \varepsilon F_c \quad (8)$$

and substituting them into Eq. (7) with $j = k = m$ only, allows the sound power for mode m to be expressed as a function of the external forces. P_{total} is real by definition, but F_1 and F_c may be complex. Taking F_1 as real and setting the derivatives $\partial P_{tot}/\partial(\text{Re}(F_c))$ and $\partial P_{tot}/\partial(\text{Im}(F_c))$ to zero in turn gives the following result for the control line forces.

$$\text{Re}(F_c) = \frac{-(a \text{Re}(\alpha\beta^*) + L \text{Re}(\gamma\epsilon^*)/2) F_1}{a|\beta|^2 + L|\epsilon|^2/2}, \quad \text{Im}(F_c) = \frac{-(a \text{Im}(\alpha\beta^*) + L \text{Im}(\gamma\epsilon^*)/2) F_1}{a|\beta|^2 + L|\epsilon|^2/2} \quad (9)$$

At a resonance, $\text{Im}(F_c)$ is small and arises from the damping included in the model, but would be more significant if this method were to be generalised to control sound power at an off-resonance frequency. Once calculated, F_c can be used with F_1 in Eq. (5) to determine A_m and C_m and hence the total sound power from the controlled cylinder using Eq. (7). While the m -terms alone give an accurate result for the uncontrolled sound power from the cylinder driven at the natural frequency of mode m , the full sums must be used for the controlled case, because many modal terms are needed for accurate spatial representation of the displacement around the line control forces.

3. RESULTS

The parameter values used to generate the following results are given in Table 1. Each added mass includes an end plate plus the annular flange it is bolted to, as shown in Fig. 1. The line force positions are based on a T-stiffener with a 100 mm flange being welded inside the cylinder 150 mm from the driven end.

Table 1. Cylinder and acoustic medium parameters.

Parameter	Value	Parameter	Value
radius, a (m)	0.2	added mass, M_1 (kg)	30
thickness, h (m)	0.002	added mass, M_2 (kg)	30
length, L (m)	1.5	line force location, d_1 (m)	0.1
density, ρ (kg/m ³)	7800	line force location, d_2 (m)	0.2
Young's modulus, E (GPa)	210	air density, ρ_o (kg/m ³)	1.21
damping factor, η	0.01	sound speed in air, c_o (m/s)	343
Poisson's ratio, ν	0.3		

The first few natural frequencies calculated (with zero damping) from the characteristic determinant of the matrix in Eq. (5) are given in Table 2. The A_m/C_m ratio shows the relative axial to radial motion, so the f_1 frequencies are for the 'concertina' axial modes of interest, while the f_2 frequencies are for radial modes. Interestingly, for the concertina modes the radial contribution increases with mode number until it equals the axial one for $m = 4$. If the end masses are set to zero, $f_1 = 1714$ Hz and $f_2 = 4369$ Hz for $m = 1$, which shows the large effect of the masses on the axial motion of the shell whose own total mass is only 29.4 kg. The 766 Hz frequency is close to the 771 Hz frequency calculated from the formula $f_n = [k_s(M_1 + M_2)/M_1M_2]^{1/2}/2\pi$ (see Blevins [16]) for two masses connected by a spring, if

$k_s = EA/L$ where A is the shell's cross-sectional area. The other f_1 frequencies almost form a harmonic series like that in axial rod vibration. The f_2 frequencies compare with the 'ring' frequency of 4328 Hz given by $f_r = c_L / 2\pi a$ with $c_L = [E/\rho(1-\nu^2)]^{1/2}$ for an infinite shell (see Fahy [15]), equivalent to $\Omega=1$ or the longitudinal wavelength equalling the circumference. Thus the radial frequencies do not change much with increasing m .

Table 2. Natural frequencies of axisymmetric modes.

m	f_1 (Hz)	A_m/C_m	f_2 (Hz)	A_m/C_m
1	766	7.71	4335	-0.026
2	1524	3.49	4359	-0.056
3	2259	1.93	4411	-0.102
4	2937	1.07	4524	-0.183

Figure 3 shows the forced response of the shell calculated from Eq. (5) with just an axial force (zero control forces) and summing 10 terms in Eq. (4). The driving-point response, Fig. 3(a), shows resonances at all four axial modes of Table 2, while the shell midpoint response, Fig. 3(b), shows only the first and third as expected. The driving-point response needed all 10 terms to converge between resonances, while the shell response only needed 5 (the response above 2259 Hz is a combination of the third and fifth modes there).

The 766 Hz mode is within the bandwidth of the inertial shakers and piezo actuators available for use on the cylinder, while the 1524 Hz mode is right at the limits. Thus discussion of radiated sound control will concentrate on these two modes. While these frequencies are relatively high in an absolute sense, the related modes are of low geometric order and so suitable for application of active control, particularly for a test-of-concept like this where the real application will be low-frequency. Table 3 gives the optimum line control forces calculated from Eq. (9) for the first three axial modes, as well as the associated uncontrolled and controlled total radiated PWL from Eq. (7). At 766 Hz, $k_0 a = 2\pi a f / c_0$ is 2.8, for and above which the piston normalised radiation resistance and shell radiation efficiency are both unity (see graphs in Bies and Hansen [14] and Fahy [15]), so Eqs. (6) and (7) are valid. Although fairly large reductions of 10 dB or more can be achieved, they come at the cost of very high control forces. For the first mode ($m=1$), the point force equivalent to a line force of magnitude $F_c = 30.8$ N/m is 38.7 N, two of which are needed: a total of 77.4 N generated to control an axial force of 1 N. This can be understood in terms of

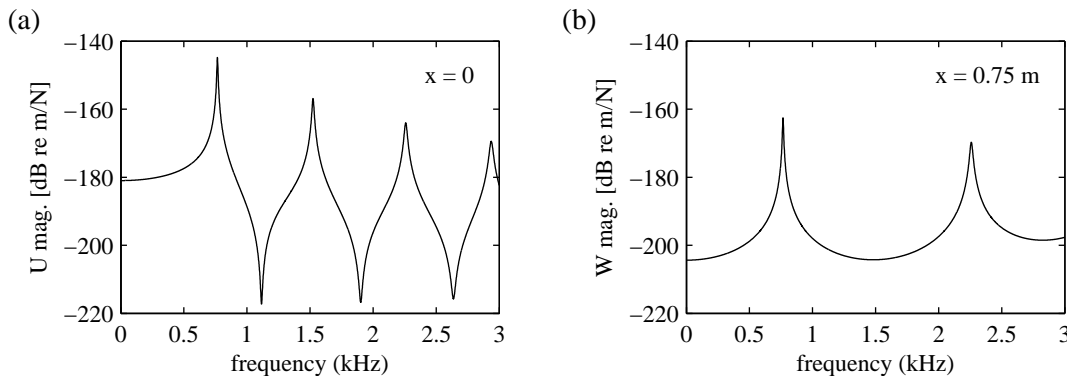


Figure 3. Magnitudes of (a) the axial displacement at the driven end of the cylinder and (b) the radial displacement in the middle of the cylinder, under axial loading only.

reciprocity if the A_m/C_m of Table 2 are considered. An axial force generates a very small radial displacement in the first axial mode, so a radial control force of the same magnitude will generate a very small axial displacement, hardly enough to cancel the large axial displacement being generated by the applied axial force. The relative thinness of the shell means that the coupling of shell bending into other directions of motion is not very strong.

Table 3. Optimum line force and uncontrolled and controlled sound power for $F_1 = 1$ N.

m	f (Hz)	F_c mag. (N/m)	F_c phase (deg.)	PWL_{free} (dB)	$PWL_{\text{controlled}}$ (dB)
1	766	30.78	179.7	66.0	50.1
2	1524	8.21	178.9	61.1	49.9
3	2259	4.21	178.1	59.2	49.6

Figures 4 and 5 show the real parts of the axial and radial displacements of the cylinder driven axially by $F_1 = 1$ N at 766 Hz and 1524 Hz respectively, calculated from Eqs. (5) and (4) with zero and optimum control forces. These can be considered ‘snapshots’ of the displacements along the cylinder’s length at time $t = 0$ and integral multiples of the period thereafter. The modal sums comprised 100 terms to achieve good spatial convergence in the controlled responses.

The analysis presented so far has only considered axisymmetric motion of the cylinder. If piezo stacks are used with a T-stiffener to provide a control moment, they will in fact be applying point forces to the shell. Such point forces have a broad wavenumber content, so

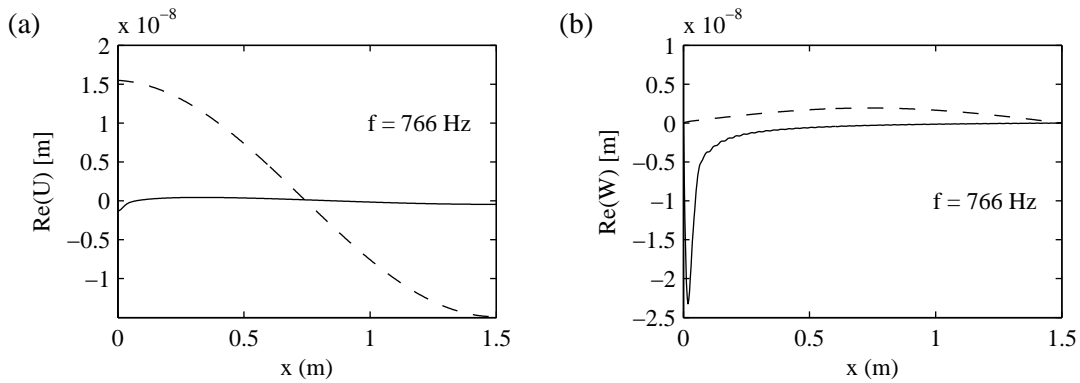


Figure 4. Real-part snapshots of (a) the axial displacement and (b) the radial displacement, uncontrolled (-----) and controlled (——) with optimum line forces, at the first resonance.

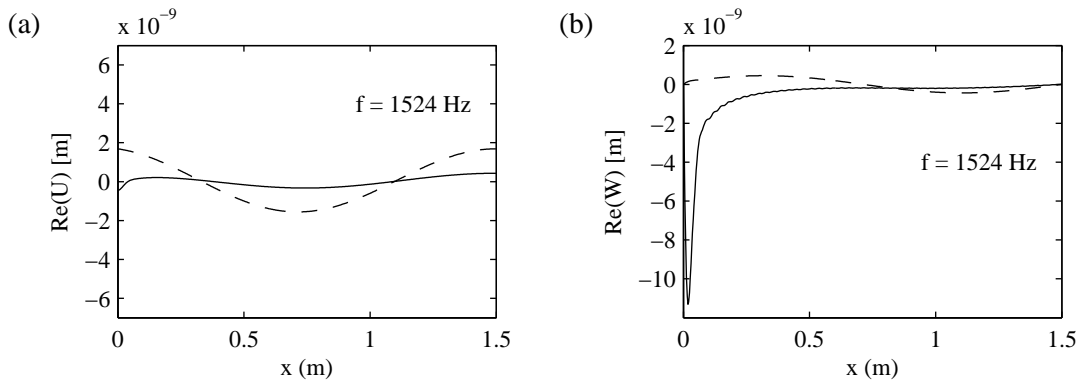


Figure 5. Real-part snapshots of (a) the axial displacement and (b) the radial displacement, uncontrolled (-----) and controlled (——) with optimum line forces, at the second resonance.

could excite higher-order modes with resonances near the driving frequency. Predominantly radial modes with $n \geq 1$ can be calculated accurately from Eq. (1) with zero forces as discussed above (see Forrest [13]). For example, radial modes (m,n) within 5% of the 766 Hz axisymmetric resonance include ones at 740 Hz (5,7), 796 Hz (1,8), 800 Hz (6,6) and 803 Hz (2,8). More exist around the 1524 Hz axisymmetric resonance. This presents a real possibility of controller ‘spillover’ (the excitation of additional modes other than that being controlled). Other considerations that have not been included in this analysis are the stiffening effect on the shell of adding a T-shaped rib, and the modes of the T-stiffener itself.

4. CONCLUSIONS

It has been shown that a modal approach is suitable for modelling the forced axisymmetric vibration of a small-scale cylindrical shell with massive end plates. For the cylinder considered, it is possible to reduce the sound power radiated by the first and second axial ‘concertina’ modes by more than 10 dB, using two circumferential line forces to provide a control moment near the driven end. However, the relative thinness of this shell means the coupling is poor and the reduction comes at the cost of very high control forces, equivalent to nearly 80 times the driving force for the first mode. There are also several higher-order modes with frequencies near the first and second axial modes, raising the possibility of controller spillover in the practical implementation of the proposed control scheme.

REFERENCES

- [1] A. Leissa, *Vibration of Shells*, Acoustical Society of America, New York, 1993.
- [2] C.H. Hodges, J. Power and J. Woodhouse, ‘The low frequency vibration of a ribbed cylinder, part 1: theory’, *Journal of Sound and Vibration*, **101**(2), 219-235 (1985).
- [3] G. Solaroli, Z. Gu, A. Baz and M. Ruzzene, ‘Wave propagation in periodic stiffened shells: spectral finite element modeling and experiments’, *Journal of Vibration and Control*, **9**(9), 1057-1081 (2003).
- [4] J.-H. Lee and J. Kim, ‘Sound transmission through periodically stiffened cylindrical shells’, *Journal of Sound and Vibration*, **251**(3), 431-456 (2002).
- [5] J.F.M. Scott ‘The free modes of propagation of an infinite fluid-loaded thin cylindrical shell’, *Journal of Sound and Vibration*, **125**(2), 241-280 (1988).
- [6] A. Harari and B.E. Sandman, ‘Radiation and vibrational properties of submerged stiffened cylindrical shells’, *Journal of the Acoustical Society of America*, **88**(4), 1817-1830 (1990).
- [7] S.-H. Choi, T. Igusa and J.D. Achenbach, ‘Nonaxisymmetric vibration and acoustic radiation of a submerged cylindrical shell of finite length containing internal substructures’, *Journal of the Acoustical Society of America*, **98**(1), 353-362 (1995).
- [8] M.H. Marcus and B.H. Houston, ‘The effect of internal point masses on the radiation of a ribbed cylindrical shell’, *Journal of the Acoustical Society of America*, **112**(3), pt 1, 961-965 (2002).
- [9] A. Himm, J. Ehrlich, H. Peine and H. Wiesner, ‘Experimental and numerical investigation of a complex submerged structure. Part I: modal analysis’, *Acta Acustica united with Acustica*, **89**(1), 61-70 (2003).
- [10] M. Blakemore, J. Woodhouse and D.J.W. Hardie, ‘Statistical power-flow analysis of an imperfect ribbed cylinder’, *Journal of Sound and Vibration*, **222**(5), 813-832 (1999).
- [11] C.R. Fuller, S.J. Elliot and P.A. Nelson, *Active Control of Vibration*, Academic Press, London, 1996.
- [12] X. Pan, Y. Tso and R. Juniper, ‘Active modal control of hull radiated noise’, *Proceedings of Acoustics 2005*, 9-11 November 2005, Busselton, Western Australia, pp. 47-53.
- [13] J.A. Forrest, ‘Measured dynamics of a thin cylindrical shell subject to axial excitation’, *Proceedings of Acoustics 2005*, 9-11 November 2005, Busselton, Western Australia, pp. 61-66.
- [14] D.A. Bies and C.H. Hansen, *Engineering Noise Control: Theory and Practice*, 2nd edition, Spon Press, London, 1996.
- [15] F. Fahy, *Sound and Structural Vibration*, Academic Press, London, 1985.
- [16] R.D. Blevins, *Formulas for Natural Frequency and Mode Shape*, Krieger Publishing Company, Malabar, Florida, USA, 1995.